Vehicle Directional Stability Control Using Bifurcation Analysis of Yaw Rate Equilibrium

M.H. ShojaeeFard[*1], S. Ebrahimi Nejad [2,] M. Masjedi[2]

1- Professor Faculty of Mechanical Engineering, Iran University of Science and Technology, Tehran, Iran 2- Faculty of Automotive Engineering, Iran University of Science and Technology, Tehran, Iran

* Corresponding Author

Abstract

In this article, vehicle cornering stability and brake stabilization via bifurcation analysis has been investigated. In order to extract the governing equations of motion, a nonlinear four-wheeled vehicle model with two degrees of freedom has been developed. Using the continuation software package MatCont a stability analysis based on phase plane analysis and bifurcation of equilibrium is performed and an optimal controller has been proposed. Finally, simulation has been done in Matlab-Simulink software considering a sine with dwell steering angle input, and the effectiveness of the proposed controller on the aforementioned model has been validated with Carsim model.

Keywords: Compensating Yaw Moment, Phase plane, Bifurcation Analysis, Optimal Control

1. Introduction

Significant research and consecutive developments have been done to enhance vehicle handling and stability. Among them, yaw moment control has proved its impact to improve handling and stability of conventional and electric vehicles under severe driving conditions [1,2]. The necessity for developing yaw moment control can be observed by examining the driver's inexperience to control the vehicle directional dynamics during critical maneuvers. For instance, in a turning maneuver with high lateral acceleration, where tire lateral forces are at the limit of road adhesion, the vehicle lateral velocity increases and the potency of the tire for generating a yaw moment is considerably reduced because of the saturation of tire lateral force. The decrease in generating yaw moment may cause an unstable motion of the vehicle, i.e. the spin out. Providing the required compensating yaw moment will therefore restore the stability of the vehicle.

For vehicle dynamics control, the yaw moment control is studied as an approach of controlling the directional motion of a vehicle during severe driving maneuvers. To meet this goal a control strategy based on the vehicle dynamics state-feedbacks, as well as an actuation system, is required. According to the present technology, the performance of vehicle dynamics control actuation mechanisms is based on the control of braking force on each wheel individually known as the differential braking that can be achieved using the main parts of the common anti-lock braking systems [3,4].

In general, design of the required control system based on the measured or estimated variables to attain the desired performance is an attracting field of research. Many researchers in the last decade have reported direct yaw moment control as one of the most effective methods, which could significantly recover the vehicle stability and controllability. They have proposed various control methods, including, optimal control [5,6], fuzzy logic control [7], H_∞ yaw-moment control [8], internal model control [9], multi-objective control [10], linear-quadratic regulator (LQR) and sliding mode control [11], etc.

This paper concerns with the optimal controller design for a nonlinear two-degree-of-freedom (2-DOF) vehicle directional dynamics model considering vehicle lateral velocity and yaw rate as state feedback variables. The focus of the paper is to design a state feedback control law based on stability regions obtained from bifurcation diagrams. Hence, this paper is organized as follows. In section 2, in order to evaluate the dynamic behavior of the vehicle, a nonlinear 2-DOF vehicle model is constructed. Then, the continuation software package MatCont is used in section 3 to perform a stability analysis based on phase plane analysis and bifurcation of equilibria, and stability regions are determined for different vehicle speeds. Next, the control problem is formulated in section 4, considering a linear 2-DOF vehicle model

as the controller model. In section 5, simulation results are shown for different steering maneuvers. Finally, conclusions are presented in section 6.

2. Vehicle and tire model

2.1. 2-DOF vehicle model for simulation

2-DOF vehicle handling model is a classical model used to define the vehicle directional motion in a turning maneuver commonly. In this system equation, vehicle longitudinal velocity is assumed constant, and tire tractive force and air resistance are ignored, as shown in Figure 1.

$$\sum F_y = ma_y \Rightarrow m(\dot{v} + ru) = (F_{yfl} + F_{yfR})\cos\delta_f + F_{yrl} + F_{yrR} \tag{1}$$

$$\sum M_z = I_z\dot{r} = a[(F_{yfl} + F_{yfR})\cos\delta_f] \\ - b(F_{yrl} + F_{yfR}) \\ + \frac{T}{2}[(F_{yfR} - F_{yfl})\sin\delta_f] + M_z$$
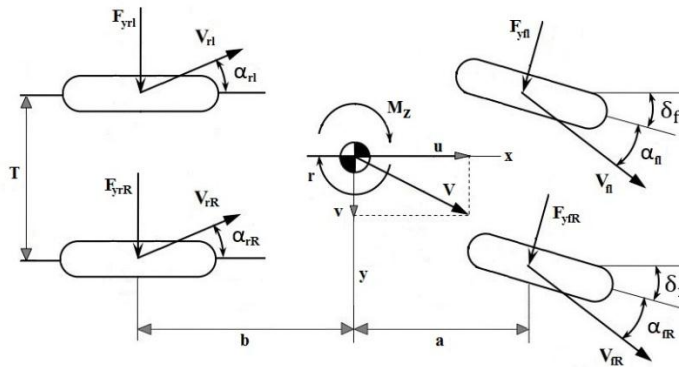

Fig1.. Plan view of the vehicle dynamics model

2.2. Tire Model

Tire lateral forces greatly affect the maneuverability of the vehicle and also have an important influence on the vehicle nonlinear dynamics system and its stability. The modeled tire is a non-linear tire based on the Pacejka Magic Formula [12], formulated as:

$$F_y = D\sin\{C\tan^{-1}[B\alpha - E(B\alpha - \tan^{-1}B\alpha)]\} \tag{2}$$

where α is the tire side slip angle and B, C, D, E are coefficients directly related to tire normal load, F_z:

$$C = 1.3$$
$$D = F_z^2 + a_2 F_z$$
$$BCD = a_3\sin(a_4\tan^{-1}(a_5 F_z)) \tag{3}$$
$$B = BCD/C/D$$
$$E = a_6 F_z^2 + a_7 F_z + a_8$$

The constants used in the above relations are listed in Table 1 [12].

An input quantity for the tire lateral force calculations is the normal load on each tire. If the vehicle is considered as a rigid body as a whole, load transfer due to the longitudinal and lateral accelerations can be determined. According to this approach that divides the load transfer in the front and rear proportional to their static loads [11], the individual normal forces are given by:

$$F_{zfl} = F_{zfs}\left(1 + 2\frac{a_y}{g}\frac{h}{T}\right) - ma_x\frac{h}{2l}$$

$$F_{zfR} = F_{zfs}\left(1 - 2\frac{a_y}{g}\frac{h}{T}\right) - ma_x\frac{h}{2l} \tag{4}$$

$$F_{zrR} = F_{zrs}\left(1 - 2\frac{a_y}{g}\frac{h}{T}\right) + ma_x\frac{h}{2l}$$

$$F_{zrl} = F_{zrs}\left(1 + 2\frac{a_y}{g}\frac{h}{T}\right) + ma_x\frac{h}{2l}$$

where the front and rear static loads are expressed as:

$$F_{zfs} = \frac{mgb}{l}$$

$$F_{zrs} = \frac{mga}{l}$$

(5)

Another variable of the tire cornering force function is the tire side slip angle, α, and can be calculated for each wheel as below [11]:

The constants used in the above relations are listed in Table 1 [12].

$$\alpha_{fl} = \tan^{-1}\left(\frac{v + ar}{u - \frac{T}{2}r}\right) - \delta_f \qquad \alpha_{rR} = \tan^{-1}\left(\frac{v - br}{u + \frac{T}{2}r}\right)$$

$$\alpha_{fR} = \tan^{-1}\left(\frac{v + ar}{u + \frac{T}{2}r}\right) - \delta_f \qquad \alpha_{rl} = \tan^{-1}\left(\frac{v - br}{u - \frac{T}{2}r}\right)$$

(6)

## 3. Phase plane analysis and bifurcation of equilibria

Using the specifications data of the case study vehicle, the phase plot at 0 radians of front steer angle is shown in Figure 2.a. These phase plots describe the propagation of the states for a relatively wide range of initial states. The red points represent solutions for equilibrium points. Equilibrium solutions are the roots of the state space equations. In other words, they are states where $\dot{v} = \dot{r} = 0$. In this plot, a stable equilibrium solution at $v = 0$ and $r = 0$ clearly exists. Stability of this solution can be qualitatively determined as multiple trajectories propagate toward this point. There also exists two saddle point equilibrium solutions. Figure 2.b shows the phase plot at 0.03 radians of front steer angle. The stable equilibrium point has migrated towards a positive

yaw rate and a negative lateral velocity. All three equilibrium points are still present. At 0.06 radians of front steer (Figure 2.c), the stable equilibrium point and one saddle point have disappeared, leaving only the other saddle point. This represents a bifurcation with respect to steer angle somewhere between 0.03 and 0.06 radians. A bifurcation is a qualitative change in the system with respect to a certain variable. In this case, the qualitative change due to increase in front wheel steer angle was a loss of two equilibrium solutions.

Figures 3.a and 3.b developed by the continuation software package MatCont [13] are the bifurcation diagrams for front steer angle as the varying parameter. Figure 3.a shows the values of lateral velocity, v, for each of the equilibrium points in the phase plot as δ_f is varied. Figure 3.b shows the corresponding diagram for yaw rate, r, as δ_f is varied. Stable equilibrium solutions are identified in solid lines, and unstable points (saddle points in this case) are identified in dotted lines. At a front steer angle of 0 radians, there are three equilibrium points. As front steer angle is increased the stable point and one saddle point converge and disappear forming a saddle node bifurcation (SN) [14]. As front steer angle is increased past the bifurcation point, only one saddle point remains in the negative yaw direction. This is unusual for a vehicle steering to the right. The negative yaw equilibrium point is unstable and relates to a "drifting" vehicle. This is a condition where the vehicle develops enough lateral velocity in the turn that steering the wheels in the opposite direction of the yaw rate will orient the wheels in the direction of velocity. Drifting is commonly thought of as an extreme case of oversteer, the phase plots show it more accurately as an unstable equilibrium condition with the vehicle turning in the opposite direction of the steer angle.

Table 1. Magic Formula Constants

a_1	-22.1
a_2	1011
a_3	1078
a_4	1.82
a_5	0.208
a_6	0
a_7	-0.354
a_8	0.707
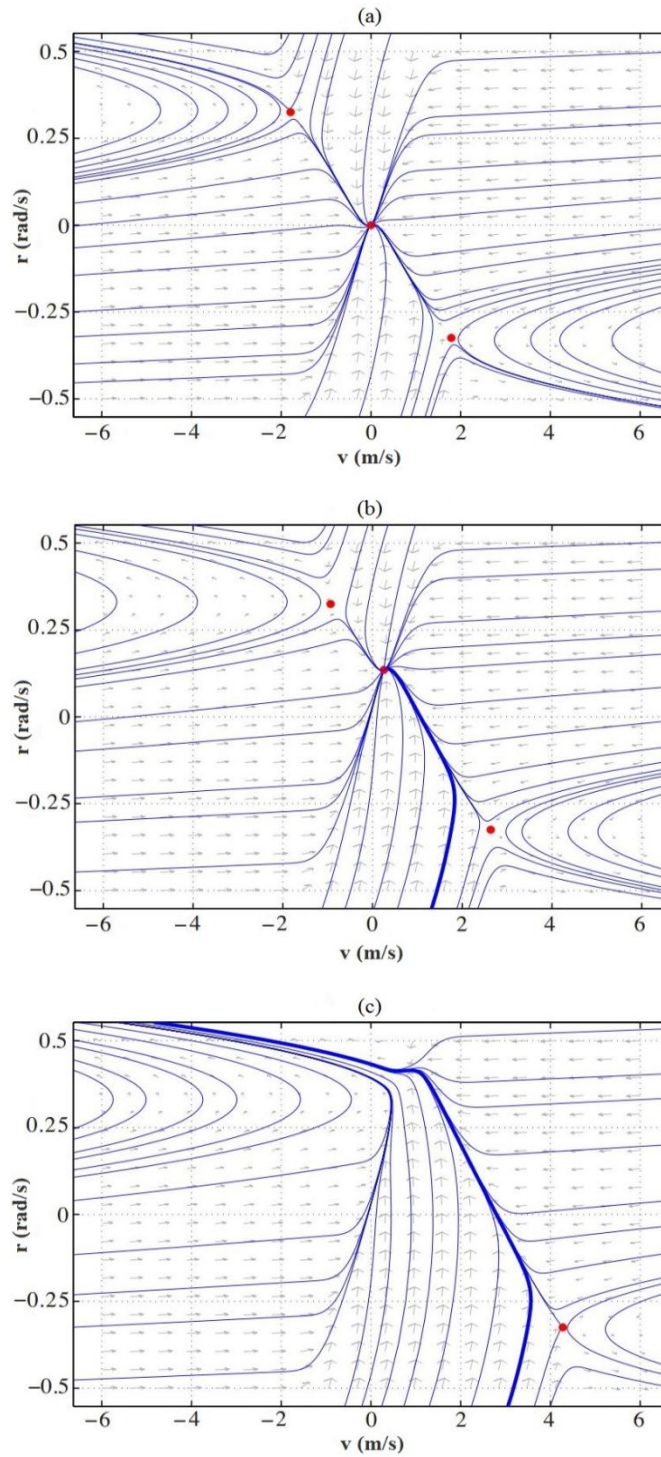
Fig2.. Phase plots at u=20 m/s;

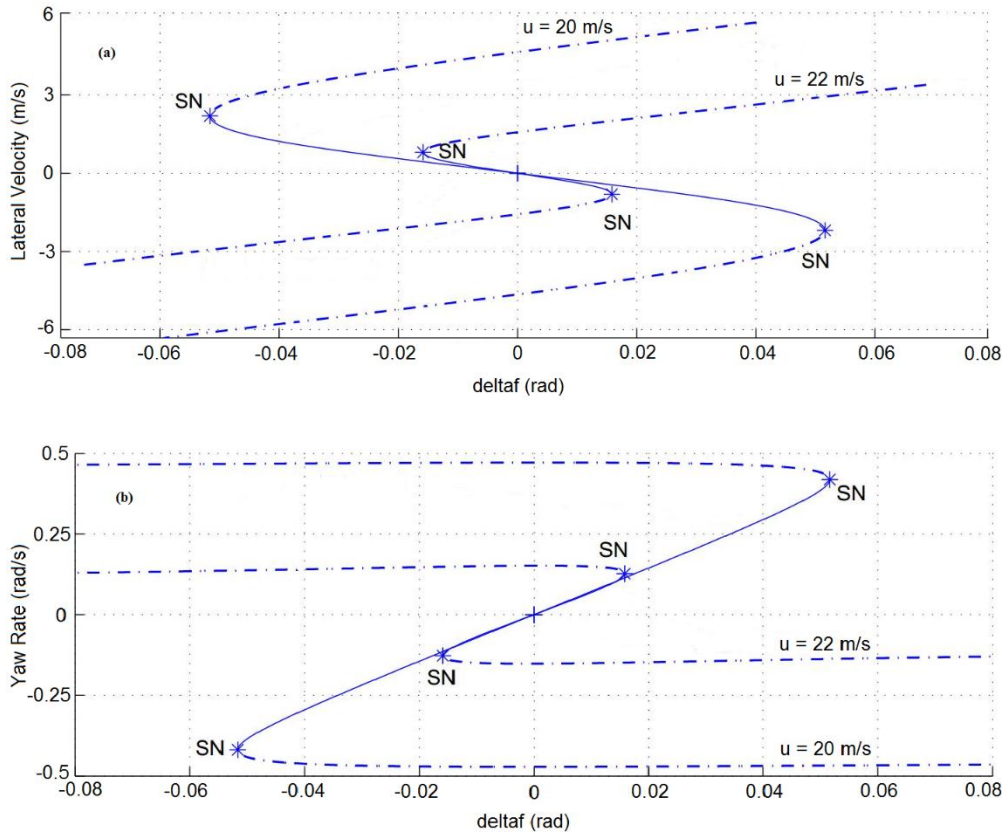(a) δ_f=0 rad, (b) δ_f=0.03 rad, (c) δ_f=0.06 rad

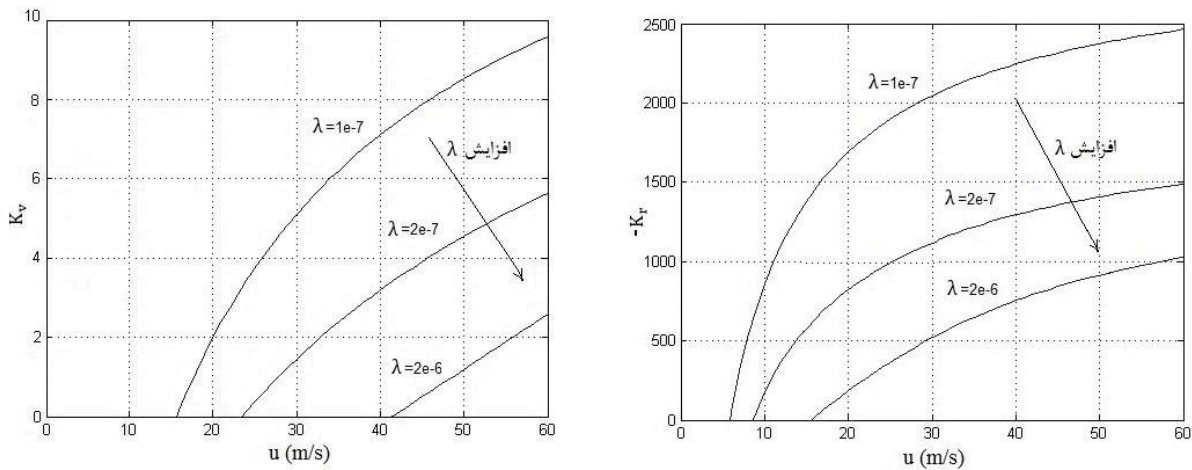**Fig3.** Bifurcation of equilibria diagrams, (a) Lateral Velocity (b) Yaw Rate

Fig4. Variations of the values of feedback gains with vehicle longitudinal velocity

4.Controller design

A commonly used linear two-degree of freedom model for vehicle handling is developed. The governing linearized equations (1) for the yaw and lateral motions of the vehicle model, in the state-space form, are derived as [11]:

$$\dot{x} = Ax + BU + E\Delta \qquad (7)$$

where

$$x = \begin{bmatrix} v \\ r \end{bmatrix}, \quad U = [M_z], \quad \Delta = [\delta_f], \quad A =$$

$$\begin{bmatrix} \frac{c_f+c_r}{mu} & \frac{ac_f-bc_r}{mu} - u \\ \frac{ac_f-bc_r}{uI_z} & \frac{a^2c_f+b^2c_r}{uI_z} \end{bmatrix}, \quad B = \begin{bmatrix} 0 \\ \frac{1}{I_z} \end{bmatrix}, \quad \text{and} \quad E = \begin{bmatrix} -\frac{c_f}{m} \\ -\frac{ac_f}{I_z} \end{bmatrix}$$

For the vehicle model, the lateral velocity, v, and the yaw rate, r, are considered as the two state variables while the yaw moment, M_z, is the control input, which must be determined from the control law. Moreover, the vehicle steering angle, δ_f, is considered as the external disturbance.

2. Optimal handling performance index 4.1.

It has been stated before that enhanced steerability and stability are the two important aspects of the optimum vehicle handling. One could hence define the cost functional or the performance index for the optimum road handling of a vehicle in the following form:

$$J = \int_0^\infty [(v - v_{bif})^2 + (r - r_{bif})^2 + \lambda M_z^2]dt \qquad (8)$$

where v_{bif} and r_{bif} are the bifurcation values of lateral velocity and the yaw rate of the vehicle obtained from figures 3.a and 3.b, respectively. In accordance to the above definition, the term $(r - r_{bif})$ in the performance index is a measure of the vehicle steerability. Minimization of this term leads the vehicle to a neutral steer and stable behavior.

4.2. Structure of the control law

The control law consists of two state variable feedback terms being those of the yaw rate and the lateral velocity. Thus the control law that minimizes the performance index in order to achieve the optimum handling behavior can be defined as:

$$M_z = K_r \Delta r + K_v \Delta v \qquad (9)$$

To determine the values of the feedback control gains, K_v and K_r, which are based on the defined performance index and the vehicle dynamic model, a LQR controller has been formulated for which its analytical solution is obtained [5]. In that case, the performance index of Eq. (8) may be rewritten in the following form:

$$J = \int_{t_i}^{t_f} [U^T R U + X^T Q X]dt \qquad (10)$$

where

$$U = [M_z], \qquad Q = \begin{bmatrix} 1 & -1 \\ 1 & 1 \end{bmatrix}, \qquad R = [\lambda], \quad \text{and} \quad X = \begin{bmatrix} v - v_{bif} \\ r - r_{bif} \end{bmatrix}$$

Considering matrices A, B, R and Q, the matrix P is found by solving the continuous-time Riccati algebraic equation. Since both controllability and observability matrices are full rank, Eq. (11) has an exclusive, symmetric and positive definite solution as follows:

$$AP^T + PA - PBR^{-1}B^TP + Q = 0 \implies P = \begin{bmatrix} P_{11} & P_{12} \\ P_{12} & P_{22} \end{bmatrix} \qquad (11)$$

The corresponding expanded equations can therefore be solved analytically in order to determine the values of the feedback gains:

$$P_{22} = \frac{1}{\alpha}\left[\eta\sqrt{\eta^2 - 2\gamma + \alpha + \sqrt{\gamma^2 + \alpha a_{11}^2}}\right] \qquad (12)$$

where

$$\eta = a_{11} + a_{22}, \qquad \gamma = a_{11}a_{22} - a_{12}a_{21}, \quad \text{and} \quad \alpha = \frac{1}{I_z^2 \lambda}$$

The other components of the matrix P can now be expressed as a function of P_{22}:

$$P_{12} = \frac{1}{2a_{12}}(\alpha P_{22}^2 - 2a_{22}P_{22} - 1) \qquad (13)$$

and

$$P_{11} = \frac{1}{2a_{12}^2}[\eta + (2\gamma + 2a_{22}^2 - \alpha)P_{22} - \alpha(a_{11} + 3a_{22})P_{22}^2 + \alpha^2 P_{22}^3] \qquad (14)$$

State feedback gain matrix is defined as:

$$K = [K_v \quad K_r] = -R^{-1}B^TP \qquad (15)$$

According to Eqs. (7) to (15), the values of the feedback gains can hence be expressed as:

$$K_v = -\frac{P_{12}}{I_z \lambda} \quad K_r = -\frac{P_{22}}{I_z \lambda} \qquad (16)$$

The variation of the optimal values of the feedback gains with the vehicle longitudinal velocity,

It can be seen from Figure 4. that the yaw rate gain K_r is always negative and its magnitude increases rapidly with the increase in vehicle longitudinal velocity u. On the other hand, the magnitude of the yaw rate gain decreases when the value of λ increased. The lateral velocity gain K_v has positive values and the variation of its magnitude with u and λ are quite similar to K_r, but its magnitude is relatively smaller than K_r to some extent that can be neglected. The values of the feedback gains found are then substituted back into Eq. (9) to obtain the optimal control law. It has been shown that the dynamic performance of the controller is extremely sensitive to the values of the weighting factor λ. Therefore, the weighting factor should be determined such that the compensating yaw moment would always remain below its admissible value to avoid wheel-lock during every cornering maneuver. As mentioned before, the external yaw moment is exerted via braking force on the wheels based on the direction of turn and whether the vehicle is over steering or under steering:

Turning right + over steering: Front-Left wheel

Turning left + over steering: Front-Right wheel

Turning left + under steering: Rear-Left wheel

Turning right + under steering: Rear-Right wheel

for different values of the weighting factor λ is shown in   Figure   4.

5. Simulation Results

Computer simulations are conducted to verify the effectiveness of the proposed controller. Simulation results are carried out using the nonlinear 2DOF vehicle model and the simulation software based on Matlab and Simulink. Figure 5 shows the structure of control system. The main goal of the control system is to make the actual yaw rate to follow the bifurcation value of yaw rate in a specific longitudinal velocity in order to prevent vehicle spin out. Another purpose is to limit magnitude of braking force to guarantee the wheel not to be locked.

Figure 6 illustrates the BSC Simulink module. This module uses differential braking to ensure that the vehicle retains its directional stability.

Figures 8 and 9 show the simulation results for vehicle behavior comparison between the proposed vehicle model and a co-simulated full vehicle model in Carsim [11]. The effectiveness of the designed controller is validated considering four different steering angle amplitudes in a sine with dwell steering maneuver shown in Figure 7. It can be observed that for both vehicle model, the responses of the yaw rate and the lateral acceleration successfully follow their desired values. Although the trends are more realistic for a full vehicle model, it is confirmed that the stability of the vehicle can significantly be guaranteed with the proposed controller. Moreover, any increase in steering wheel angle amplitude will lead to increase in yaw rate difference and consequently increase in braking force on tire. This procedure can finally cause a decrease in performance of controller as it is well seen in higher amplitudes.
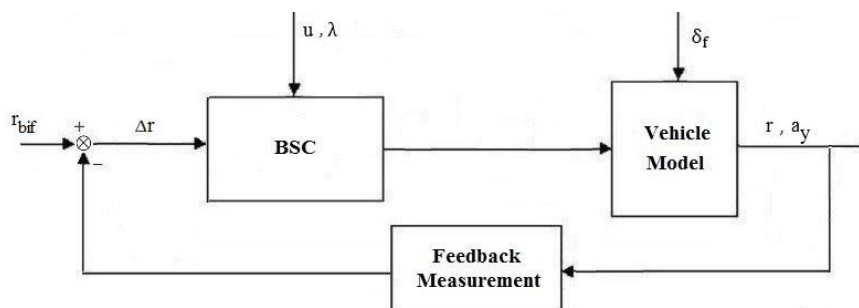

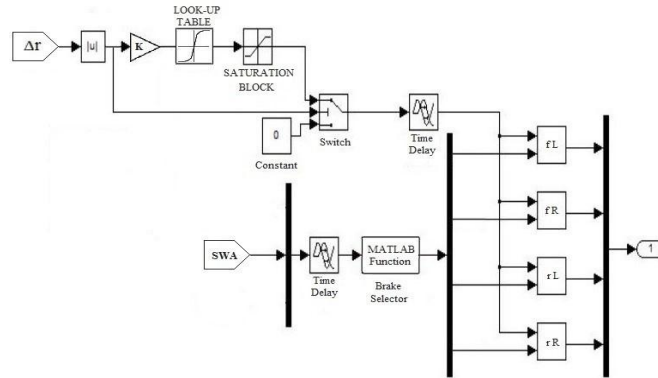**Fig5.** Block diagram of control system
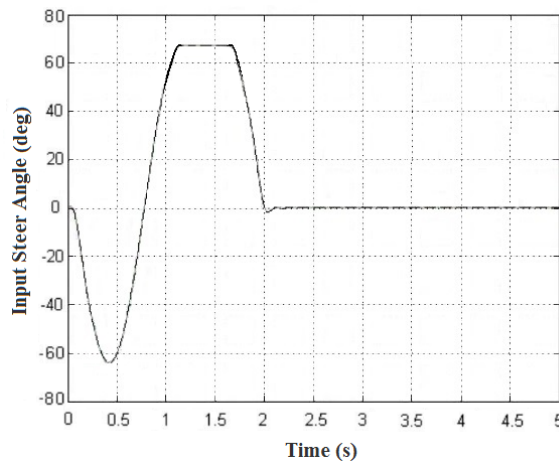
Fig6.BSC Simulink module

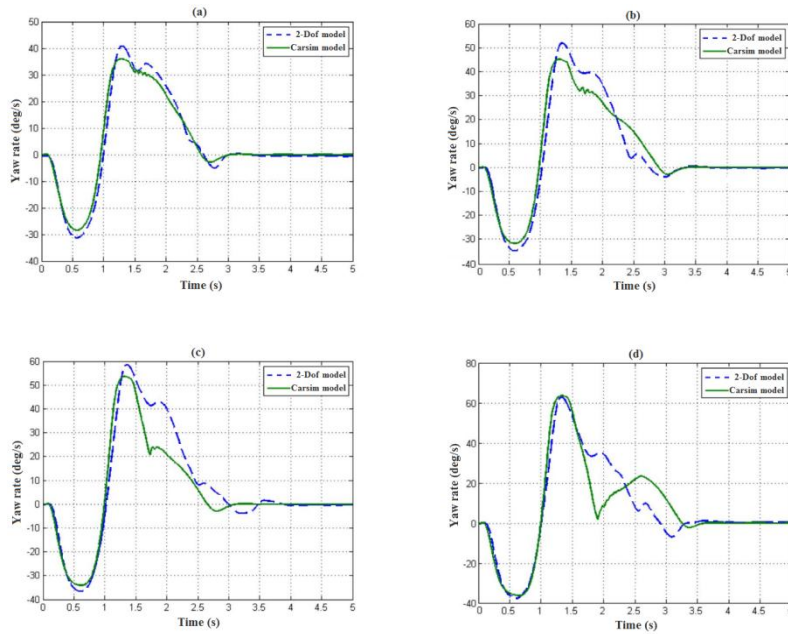**Fig7.**Steering input for a sine with dwell maneuver

Fig8.. Variation of validated yaw rate for different steering wheel angle amplitudes;
δ_{sw}=75 deg, (b) δ_{sw}=80 deg, (c) δ_{sw}=85 deg, (d) δ_{sw}=90 deg
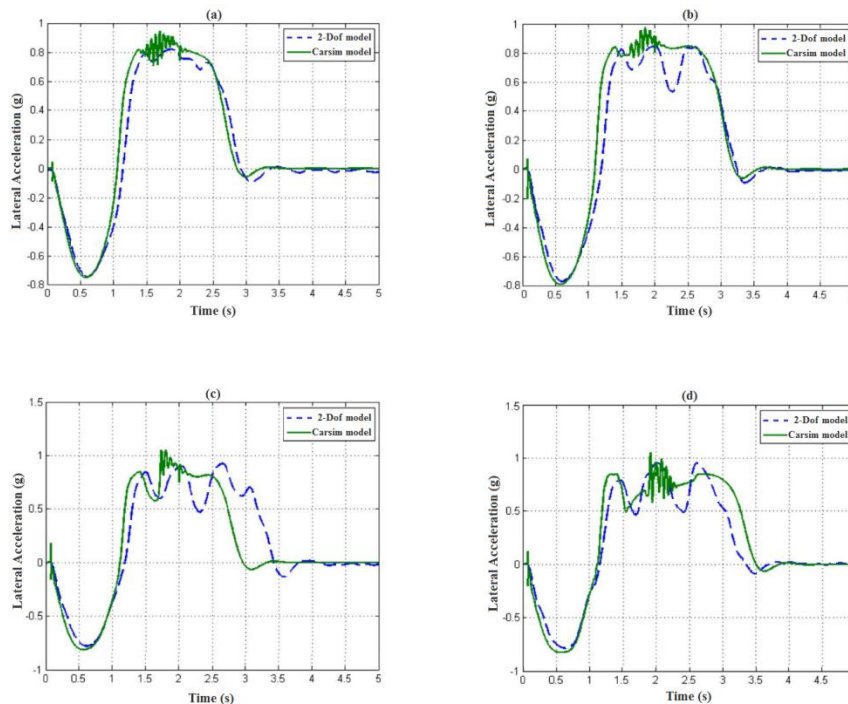
Fig9. Figure 9. Variation of validated lateral acceleration for different steering wheel angle amplitudes;

(a) δ_{sw}=75 deg, (b) δ_{sw}=80 deg, (c) δ_{sw}=85 deg, (d) δ_{sw}=90 deg

6. Conclusion

The control algorithm used in this work in order to stabilize the vehicle under unstable conditions, uses a concept similar to that of other available controllers used in vehicle dynamics control systems with two considerable difference. The proposed optimal controller can be equipped with a stable region instead of tracking the control variables at any time. The data of stability regions are obtained from a bifurcation of equilibria analysis. In the meantime, by proper selection of the weighting factor and an appropriate design of the control law, in order to minimize the performance index, not only an excellent handling behavior is achieved, but also physical limits like wheel lock are also satisfied.

References

[1]. L. De Novellis, A. Sorniotti, P. Gruber, J. Orus, J.-M. Rodriguez Fortun, J. Theunissen, et al., 2015, Direct yaw moment control actuated through electric drivetrains and friction brakes: Theoretical design and experimental assessment, Mechatronics, 26: 1-15.

[2]. Y. F. Lian, X. Y. Wang, Y. Zhao, and Y. T. Tian, 2015, Direct Yaw-moment Robust Control for Electric Vehicles Based on Simplified Lateral Tire Dynamic Models and Vehicle Model, IFAC-PapersOnLine, 48: 33-38.

[3]. J. Lee, J. Choi, K. Yi, M. Shin, and B. Ko, 2014, Lane-keeping assistance control algorithm using differential braking to prevent unintended lane departures, Control Engineering Practice, 23: 1-13.

[4]. Q. Lu, P. Gentile, A. Tota, A. Sorniotti, P. Gruber, F. Costamagna, et al., 2016, Enhancing

[5]. vehicle cornering limit through sideslip and yaw rate control, Mechanical Systems and Signal Processing, IN PRESS.

[6]. E. Esmailzadeh, A. Goodarzi, and G. R. Vossoughi, 2003, Optimal yaw moment control law for improved vehicle handling, Mechatronics, 13: 659-675.

[7]. M. Eslamian, G. Alizadeh, and M. Mirzael, 2007, Optimization-based non-linear yaw moment control law for stabilizing vehicle lateral dynamics. Proc. Instn. Mech. Engrs. Part D, 221:1513-1523.

[8]. B. L. Boada, M. J. L. Boada, and V. Díaz, 2005, Fuzzy-logic applied to yaw moment control for vehicle stability. Vehicle System Dynamics, 43:753-770.

[9]. R. Wang, H. Jing, C. Hu, M. Chadli, and F. Yan, 2016, Robust H∞ output-feedback yaw control for in-wheel motor driven electric vehicles with differential steering, Neurocomputing, 173 (3): 676-684.

[10]. M. Canale, L. Fagiano, M. Milanese, and P. Borodani, 2007, Robust vehicle yaw control using an active differential and IMC techniques. Control Engineering Practice, 15:923-941.

[11]. H.M. Lv, N. Chen, and P. Li, 2004, Multi-objective H_∞ optimal control for four-wheel steering vehicle based on yaw rate tracking. Proc. Instn. Mech. Engrs. Part D, 218:1117-1123.

[12]. S. Zhang, H. Tang, Z. Han, and Y. Zhang, 2006, Controller design for vehicle stability enhancement. Control Engineering Practice, 14: 1413-1412.

[13]. H. B. Pacejka, 2012, Tire and Vehicle Dynamics, Third Edition, Butterworth-Heinemann (Elsevier), Oxford.

[14]. A. Dhooge, W. Govaerts, Yu.A. Kuznetsov, H.G.E. Meijer and B. Sautois, 2008, New features of the software MatCont for bifurcation analysis of dynamical systems, Mathematical and Computer Modelling of Dynamical Systems, 14 (2): 147-175.

[15]. S. Inagaki, I. Kshiro, M. Yamamoto, 1994, Analysis on vehicle stability in critical cornering using phase-plane method. Proceedings of AVEC'94, Tsukuba, Japan.